State-Resolved Time-Dependent Wave Packet and Quasiclassical Trajectory Studies of the Adiabatic Reaction S(P-3) + HD on the (1(3)A '') State

ARTICLE *in* THE JOURNAL OF PHYSICAL CHEMISTRY A · DECEMBER 2013

Impact Factor: 2.69 · DOI: 10.1021/jp410868v · Source: PubMed

3 AUTHORS, INCLUDING:

Jiuchuang Yuan
Dalian University of Technology
10 PUBLICATIONS **26** CITATIONS

SEE PROFILE

THE JOURNAL OF PHYSICAL CHEMISTRY A

Article

pubs.acs.org/JPCA

State-Resolved Time-Dependent Wave Packet and Quasiclassical Trajectory Studies of the Adiabatic Reaction S(^{3}P) + HD on the (1^{3}A″) State

Dahai Cheng, Jiuchuang Yuan, and Maodu Chen*

School of Physics and Optoelectronic Technology, and College of Advanced Science and Technology, Dalian University of Technology, Dalian 116024, People's Republic of China

ABSTRACT: Time-dependent wave packet (TDWP) and quasiclassical trajectory (QCT) calculations have been carried out for the reaction S(^{3}P) + HD($X^1\Sigma_g^+$) at the lowest 1^{3}A″ state with both rotational and vibrational excitations of reactant HD. The calculated integral cross sections from QCT agree fairly well with the TDWP calculations. The reaction probability results from TDWP show that the reaction displays a strong tendency to the SD channel. When the reactant HD is vibrationally excited, both channels are promoted apparently. The vibration of the HD bond tends to reduce the difference of reactivity between the two channels. The detailed state-to-state differential cross sections (DCSs) are calculated. These distributions show some significant characters of the barrier-type reactions. At the same time, the scattering width of product SD has a certain relationship with its rotation excitation. For the vector properties, $P(\theta_r)$, $P(\phi_r)$, and $P(\theta_r,\phi_r)$ distributions are calculated by QCT, and the increased collision energy weakens the rotational polarization of the SD molecule.

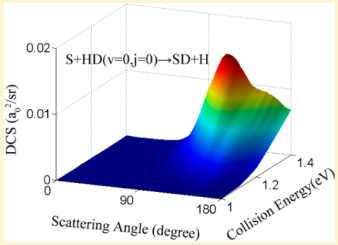

1. INTRODUCTION

The sulfur atom and its chemical compounds are important in combustion and atmospheric chemistry. Recently, the reaction of the SH_2 system and its isotopic substituted reactions has been studied frequently in both theory and experiment.[1−3] The S(^{3}P) + H_2 reaction is the simplest triatomic reaction involving sulfur atoms, and it is a paradigm for the hydrogen atom abstraction reaction.

Most of the earlier studies focus on S(^{1}D) + H_2 and intersystem crossing reactions. Lara et al. studied the S(^{1}D) + H_2 → SH + H reaction in kinetics and took the crossed-beam experiment at a very low collision energy.[3−5] Their consistent results in simulation and experiment explained that the excitation function behavior is the cumulative contribution of various partial waves. Yang et al. studied the S(^{1}D) + HD reaction on the ground adiabatic electronic state, and they calculated the reaction integral and differential cross sections (DCSs) and also investigated the Coriolis coupling using the DRW code.[6,7] Ho et al. structured a potential surface of the 1A′ state for the S(^{1}D) + H_2 reaction by global ab initio calculations, which shows improvement over other earlier work.[8] The stereodynamics study was also carried out between S(^{1}D) + H_2 and S(^{1}D) + HD reactions by Su and Kang using the QCT method.[9]

The resent studies mentioned above all focus on the ^{1}D state sulfur. However, the S(^{3}P) + H_2 reaction is often investigated on the singlet−triplet crossing effects. We know that S(^{3}P) correlates to three triplet potential energy surfaces, which are of 1^{3}A″, 2^{3}A″, and ^{3}A′ states for the SHH system. The excited reagent S(^{1}D) with H_2 correlates with the ground-state product on the ^{1}A′ state. Earlier studies on the spin-forbidden decomposition provided hints of the spin−orbit coupling.[10,11] After that, Maiti et al. made a detailed study on the S(^{3}P,^{1}D) + H reaction through the determination of global potential energy surfaces and spin−orbit couplings using a trajectory surface-hopping method.[12] They found that the intersystem crossing occurs and affects both the S(^{3}P) + H_2 and S(^{1}D) + H_2 reactions. The S(^{3}P) + H_2 reaction even occurs without surmounting the triplet barrier. Nowadays, the TDWP has become an effective method to investigate the nonadiabatic effect in chemical dynamics for more accurate results.[13,14] After the typical O + H_2 reaction,[15] Chu took a more accurate study of the nonadiabatic effect in the S(^{1}D) + HD reaction using the TDWP method. The results show a discrepancy of isotope effects between theoretically calculated and experimentally measured, which also can be attributed to nonadiabatic effects.[16]

Although nonadiabatic effects are important for the S + H_2 reaction, adiabatic dynamics study is needed, not only for making more detailed understanding of this reaction but also for further investigations on intersystem crossing. This paper focuses on the state-to-state reactive dynamics study and the stereodynamics study of the isotopic reaction S(^{3}P) + HD using the time-dependent wave packet (TDWP) method[17] and quasiclassical trajectory (QCT) method[18] via a potential energy surface newly fitted by Lv[2]. This paper is organized as follows. In section 2, we briefly describe the theory that we used in the calculations. Section 3 gives our detailed results and discussions. The conclusions are presented in section 4.

Received: November 4, 2013
Revised: December 8, 2013
Published: December 12, 2013

   dx.doi.org/10.1021/jp410868v | J. Phys. Chem. A 2014, 118, 55−61

2. THEORY

Time-Dependent Wave Packet (TDWP) Calculation. In this work, we use the reactant Jacobi coordinates in the body-fixed (BF) representation and propagate the wave packet using the second-order split operator (SO) algorithm.[19−21] In the reactant Jacobi coordinates, the Hamiltonian can be written as

$$\hat{H} = -\frac{\hbar^2}{2\mu_R}\frac{\partial^2}{\partial^2 R} + \frac{(J-j)^2}{2\mu_R R^2} + \frac{j^2}{2\mu_r r^2} + V(R, r, \gamma) + h(r)$$

R and r are defined as the distances of S−HD and H−D, respectively, and γ is the enclosing angle of them. μ_R and μ_r are the reduced masses associated with R and r coordinates, respectively. V corresponds to the potential energy of this system; in this work, we use the adiabatic surface in $1^3A''$ state, which was fitted by Lv recently. $h(r)$ is the reference Hamiltonian defined by

$$\hat{h}(r) = -\frac{\hbar^2}{2\mu_r}\frac{\partial^2}{\partial^2 r} + \nu(r)$$

with $\nu(r)$ being the diatomic potential function.

The Hamiltonian was discretized using mixed finite basis representation and discrete variable representation (FBR and DVR),[22] the DVR for radial degrees of freedom and the FBR of spherical harmonic basis for angular degrees of freedom.

The SO scheme[19,23] is used to propagate the initial wave packet on the potential energy surface

$$\psi^{JM\epsilon}(R, r, \gamma, t + \Delta) = e^{-iH_0\Delta/2}e^{-iU\Delta}e^{-iH_0\Delta/2}\psi(R, r, \gamma, t)$$

where H_0 is the reference Hamiltonian and U is the effective potential

$$\hat{H}_0 = -\frac{\hbar^2}{2\mu_R}\frac{\partial^2}{\partial^2 R} + h(r)$$

$$\hat{U} = \frac{(J-j)^2}{2\mu_R R^2} + \frac{j^2}{2\mu_r r^2} + V(R, r, \gamma)$$

where the wave packet is expended in terms of basis $u_n^{\nu}(R)\phi_{\nu}(r)$ $Y_{jK}^{JM\epsilon}(R,r,\gamma)$ in the BF, where n and ν quantum numbers label the translational and vibrational eigenfunctions and M and K are the projection quantum numbers of the total angular momentum J on the space-fixed z axis and BF z axis, respectively, and $\epsilon = (-1)^{j_0+l_0}$ is the parity of the system. To get converged results, in this expansion, we have used 179 translational basis functions covering the range $0.1 \le R \le 18.0$ a_0, 119 vibrational basis functions covering the range $0.1 \le r \le 17.0$ a_0, and rotational basis functions up to $j_{max} = 100$. Moreover, the propagation time has been set to 8000 au. All calculations have been done using the coupled channel (CC) approximation for $J = 0$−50. Then, the state-to-state scattering matrix $S^{J\epsilon}_{\nu jK\leftarrow\nu_0 j_0 K_0}(E)$ in the helicity representation is extracted by the reactant−product decoupling (RPD) approach.[24,25] (ν_0 j_0K_0) is the quantum number of the initial state of the scattering wave function.

The helicity-averaged state-resolved reaction probability for a given value of total J and total E is defined by[26]

$$P^J_{\nu j\leftarrow\nu_0 j_0} = \frac{1}{2j_0+1}\sum_{K,K_0}|S^J_{\nu jK\leftarrow\nu_0 j_0 K_0}|^2$$

The state-to-state integral cross sections (ICSs) are obtained by[26]

$$\sigma_{\nu j\leftarrow\nu_0 j_0} = \frac{\pi}{(2j_0+1)k^2_{\nu_0 j_0}}\sum_K\sum_{K_0}\sum_J(2J+1)|S^J_{\nu jK\leftarrow\nu_0 j_0 K_0}|^2$$

and the state-to-state DCSs[26]

$$\frac{d\sigma_{\nu j\leftarrow\nu_0 j_0}(\theta, E)}{d\Omega} = \frac{1}{(2j_0+1)}\sum_K\sum_{K_0}\left|\frac{1}{2ik_{\nu_0 j_0}}\sum_J(2J+1)d^J_{KK_0}(\theta)S^J_{\nu jK\leftarrow\nu_0 j_0 K_0}\right|^2$$

in which θ is the scattering angle.

Quasiclassical Trajectory (QCT) Calculation. The QCT method is also employed in this work for comparative analysis and stereodynamic studies. A standard QCT calculation[27−30] was taken in the center-of-mass (CM) frame for reaction S + HD($\nu = 0, j = 0$) → SD + H in the range from 0.9−1.4 eV with a time integration step of 0.1 fs on the same $1^3A''$ PES, and 500 000 trajectories were sampled for each energy level.

The CM frame used in this work, where the z axis is parallel to the reagent relative velocity $\boldsymbol{k}$, and the y axis is perpendicular to the plane containing $\boldsymbol{k}$ and $\boldsymbol{k}'$; $\boldsymbol{k}'$ is the relative velocity of products.

The distribution function of the vector correlations between $\boldsymbol{k}$ and $\boldsymbol{j}'$ ($\boldsymbol{j}'$ is the angular momentum of product SD) is expanded in a series of Legendre polynomials[31,32]

$$P(\theta_r) = \frac{1}{2}\sum_l [l]a_0^{(l)}P_l(\cos\theta_r)$$

where θ_r is the angle between $\boldsymbol{j}'$ and $\boldsymbol{k}$. The coefficients $a_0^{(l)}$ are called polarization parameters, and $a_0^{(l)} = \langle P_l(\cos\theta_r)\rangle$ are the average over all of the reactive trajectories.

The dihedral angle distribution $P(\phi_r)$, which describes the $\boldsymbol{k}$−$\boldsymbol{k}'$−$\boldsymbol{j}'$ correlations can be expanded in Fourier series as[31,32]

$$P(\phi_r) = \frac{1}{2\pi}(1 + \sum_{\text{even},n>2} a_n\cos n\phi_r + \sum_{\text{odd},n\ge 1} b_n\sin n\phi_r)$$

where $a_n = 2\langle\cos n\phi_r\rangle$ and $b_n = 2\langle\sin n\phi_r\rangle$, the average over all of the reactive trajectories. To get a fine convergence in the calculation of this work,$P(\theta_r)$ is expanded up to $l = 18$ while $P(\phi_r)$ is expanded up to $n = 24$.

The $P(\theta_r,\phi_r)$ distribution can be defined as[31,32]

$$P(\theta_r, \phi_r) = \frac{1}{4\pi}\sum_k\sum_{q\ge 0}[k][a^k_{q\pm}\cos(q\phi_r) - a^k_{q\mp}i\sin(q\phi_r)]C_{kq}(\theta_r, 0)$$

The polarization parameter a^k_q is given by

$$a^k_{q\pm} = 2\langle C_{k|q|}(\theta_r, 0)\cos(q\phi_r)\rangle \qquad \text{k is even}$$

$$a^k_{q\mp} = 2i\langle C_{k|q|}(\theta_r, 0)\sin(q\phi_r)\rangle \qquad \text{k is odd}$$

In this work, $P(\theta_r,\phi_r)$ is expended up to $k = 7$ to get a good convergence.

dx.doi.org/10.1021/jp410868v | J. Phys. Chem. A 2014, 118, 55−61

3. RESULTS AND DISCUSSION

The S(^{3}P) + HD reaction on $1^3A''$ has two channels, the reaction with the product SH and the reaction with the product SD. Figure 1 presents the calculated TDWP reaction

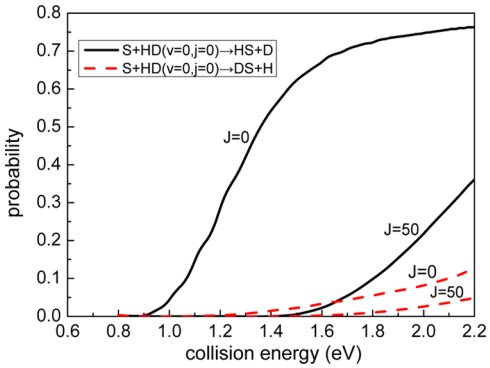

Figure 1. The reaction probabilities ($J = 0$, $J = 50$) of the S + HD($\nu = 0,j = 0$) → SD + H and S + HD($\nu = 0,j = 0$) → SH + D reaction calculated by TDWP.

probabilities (at $J = 0$, $J = 50$) as a function of collision energy for both S + HD($\nu = 0,j = 0$) → SD + H and S + HD($\nu = 0,j = 0$) → SH + D reactions. For the symmetry form of this PES, the SH and SD channels undergo almost the same reaction path. However, the reaction probabilities of these two channels are quite different. We notice that the SD + H form combination has a smaller reduced mass, which means that the relative motion between the SD and H atom is more active than that between SH and the D atom, and this reduced mass effect is particularly apparent for this abstract reaction. Therefore, in Figure 1, the SD channel shows significant advantages in reactivity. Because SD is the main product of the title reaction, the subsequent research on ICSs, DCSs, and the product polarizations only focus on this active channel.

Figure 2 presents the calculated QCT and TDWP exciting functions of the reaction S + HD($\nu = 0,j = 0$) → SD + H. We take notice that the ICSs from both QCT and TDWP methods have similar ascending trends with the increasing of collision energy from 0.9 to 1.4 eV. It is a reflection of this ($1^3A''$) PES, which has only a barrier on the reaction coordinate. The QCT curve coincides well with the TDWP calculation, as we can see

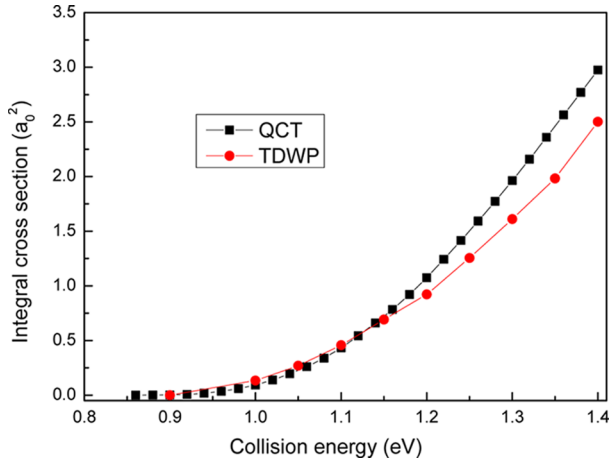

Figure 2. The QCT and TDWP reaction ICSs of the S + HD($\nu = 0,j = 0$) → SD + H reaction as a function of collision energy.

from Figure 2. Both of the curves are smooth, and no obvious quantum effect, such as tunneling and resonance, is reflected from the curves.

The reactions with a vibrationally and rotationally excited reactant are investigated by the TDWP method. Figure 3 shows

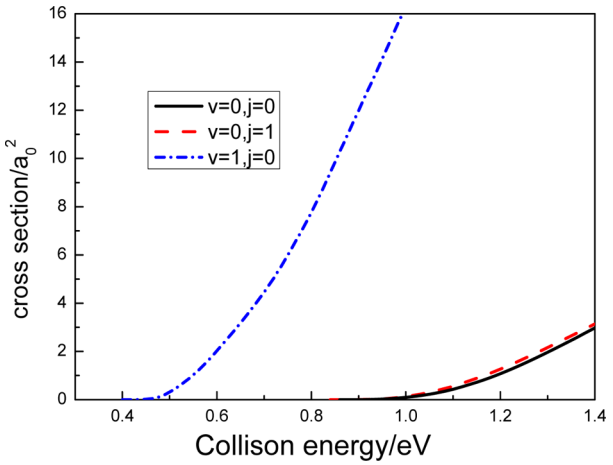

Figure 3. The ICS of the S + HD → SD + H reaction with the HD initial state of ($\nu = 0,j = 0$), ($\nu = 1,j = 0$), and ($\nu = 0,j = 1$) as a function of collision energy calculated by TDWP.

the exciting function of the reaction S + HD → SD + H with the reactant HD in rovibrational states. Compared with rotational excitation, the vibrational excitation increases the reaction activity more obviously.

The vibrationally excited reactant not only lowers the threshold by transferring the internal energy to the collision system, it also makes the ICS increase faster with the collision energy. According to the classic theory by Polanyi,[33] the major reason for this phenomenon is that the late barrier in the minimum reaction path of this ($1^3A''$) state PES[34] makes the reaction more sensitive to the vibration of the HD bond.

The vibrational excitation of HD not only promotes the reaction probability of the channel S + HD → SD + H, it also reduces the ICS gaps of the two channels. Figure 4 shows the relationship between thermal excitation and ICS ratios of the two channels. The y axis value calculated by TDWP is the cross section ratio of the SD channel to the SH channel (ICS_{SD}/

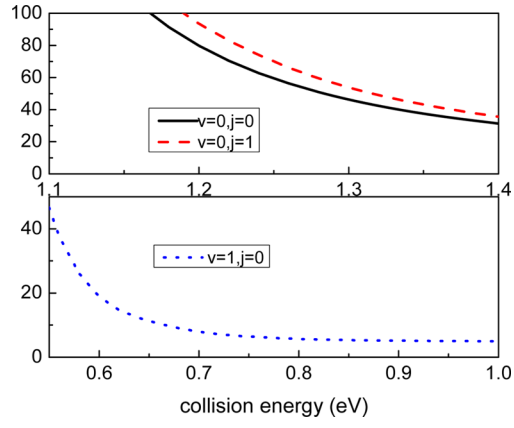

Figure 4. The effect of thermal excitation on the ICS ratio of the two channels calculated by TDWP. The y axis is the ICS ratio of the SD channel to SH channel.

dx.doi.org/10.1021/jp410868v | J. Phys. Chem. A 2014, 118, 55−61

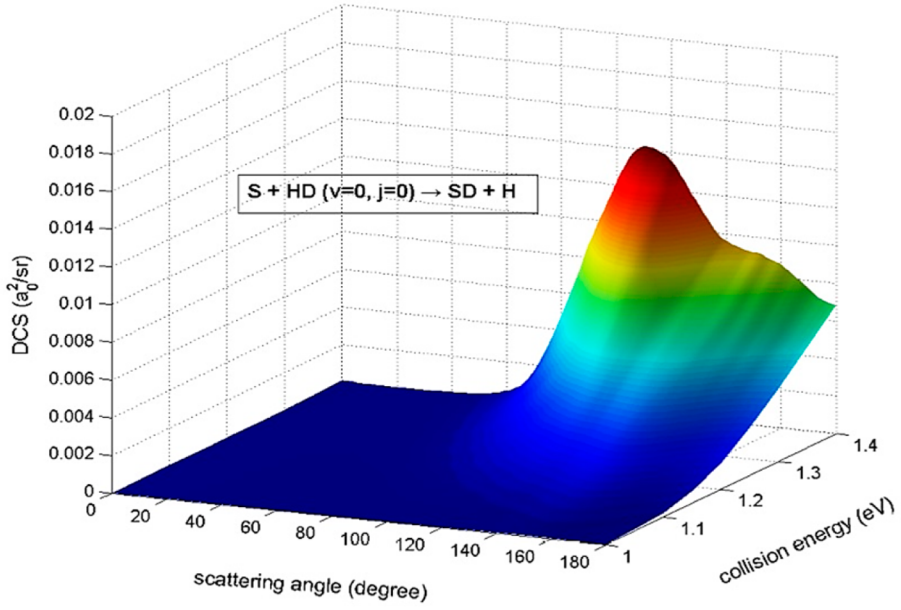

Figure 5. DCSs as a function of the scattering angle at different collision energies for the reaction S + HD(ν = 0,j = 0) → SD + H calculated by TDWP.

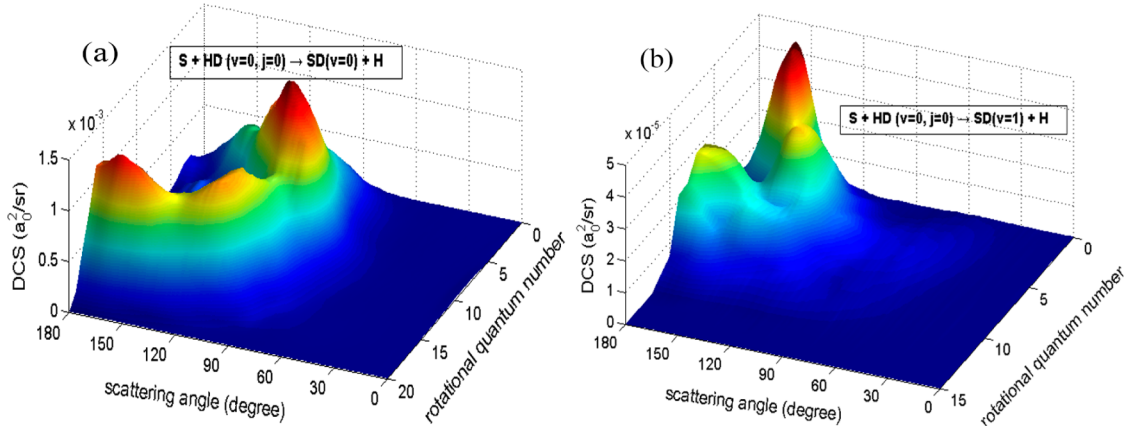

Figure 6. State-resolved DCSs as a function of scattering angle for different product states at 1.4 eV. (a) For the reaction S + HD(ν = 0,j = 0) → SD(ν = 0) + H and (b) for the reaction S + HD(ν = 0,j = 0) → SD(ν' = 1) + H calculated by TDWP.

ICS_{SH}), which reflects the ICS gap between the two channels. As the collision energy increases, the ratio value goes down and does not vary too much. As the energy gets larger, the reaction with a rotationally excited reactant has the largest ratio value (the minimum value is about 35), followed by the ground-state reaction (the minimum value is about 30), and the vibrationally excited reaction has the smallest ratio value (the minimum value is about 5). It demonstrates that the vibrationally excited reactant will reduce the gap between two channels, and the rotationally excited reactant will enlarge their gap in ICS.

Because SD is the main product of the title reaction, the subsequent research only focuses on the SD channel. The state-resolved DCS of the reaction S + HD(ν = 0,j = 0) → SD + H is investigated. Figure 5 is the 3D plot presenting the DCSs as a function of the scattering angle at different collision energies ranging from 1.0 to 1.4 eV. This reaction presents the typical characteristics of barrier-type reactions. When the collision energy is low, the reaction is dominated by a rebound module. The S atom does not have enough energy to make the reactions happen at a large collision parameter; therefore, more products are backward scattering. As the energy increases, this reaction changes to an abstraction module. The S atom can take away the D atom from HD at a larger collision parameter and makes the product side scattering.

The maximal calculated total angular momentum is J = 50, to which the reaction is converged at the collision energy of 1.4 eV. At 1.4 eV, we find that the product SD in the reaction with the ground-state reactant has only two vibrational states, ν' = 0 and 1. For these two vibrational states, there are 20 rotational states for ν' = 0 and 13 rotational states for ν' = 1. The state-resolved DCSs as a function of scattering angle for each product state at 1.4 eV are shown in Figure 6a and b. Comparing (a) and (b), we can see that most of the products are in the vibrational ground state. Interestingly, both of the two figures have the DCSs distributed along a circle arc in the x−y plain, and this can be explained by the collision energy distribution. The total collision energy can be distributed to two parts, the translational energy and the internal energy of product SD, and it can be expressed as $E_C = E_T + E_I$. To the products with high rotational states, more collision energy is

dx.doi.org/10.1021/jp410868v | J. Phys. Chem. A 2014, 118, 55−61

transferred to the SD molecule, and these reactions have small translational energy. We know that in the barrier-type reactions, a small translational energy will cause a large scattering angle, and when the translational energy gets larger, the angle will get smaller. Therefore, we can see from the two pictures that products with high rotational states are back scattering, and when the quantum number decreases, these products have high translational energy and become more front scattering. Moreover, we find that there has a sharp peak when $j = 0$ in both pictures. However, when the quantum number gets larger, the DCS distribution becomes more diffused. We suppose that the transfer process of internal energy has an impact on the reactive scattering.

We also calculated the vector properties of the reaction S + HD → SD + H. Figure 7a shows its $P(\theta_r)$ distribution, which

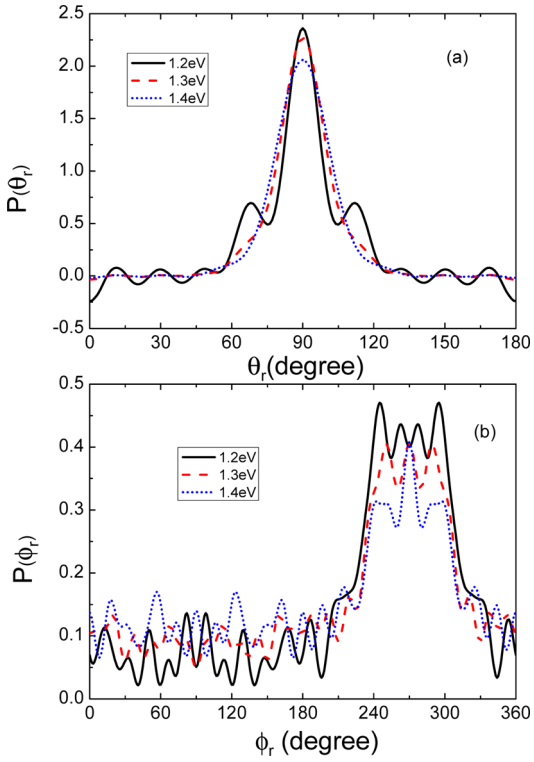

Figure 7. The angular momentum polarization distributions of (a) $P(\theta_r)$ and (b) $P(\phi_r)$ at 1.2, 1.3, and 1.4 eV for the reaction S + HD(ν = 0,j = 0) → SD + H calculated by QCT.

describes the $\boldsymbol{k}$ and $\boldsymbol{j}'$ correlations. This distribution has a symmetrical form with respect to $\theta = 90°$, and the peak at around $\theta = 90°$ can demonstrate that $\boldsymbol{j}'$ has a cylindrical symmetry distribution in the product scattering frame and the vector of $\boldsymbol{j}'$ prefers to be perpendicular to $\boldsymbol{k}$. When the collision energy gets larger, the peak gets lower, which indicates that the products' polarization is weakened. The $P(\phi_r)$ distribution that describes the $\boldsymbol{k}$–$\boldsymbol{k}'$–$\boldsymbol{j}'$ correlations is shown in Figure 7b. This distribution tends to be asymmetric with respect to the $\boldsymbol{k}$–$\boldsymbol{k}'$ scattering plane. The peak in the distribution at angles close to 270° implies a preference for left-handed product rotation in planes parallel to the scattering plane. When the collision energy increases, the peak gets lower, which means that the rotational polarization in this direction is weakened.

Figure 8 shows the $P(\theta_r,\phi_r)$ distribution at different collision energies, (a) 1.2, (b) 1.3, and (c) 1.4 eV. Through it, we can obtain the image of the SD products' polarizations and their

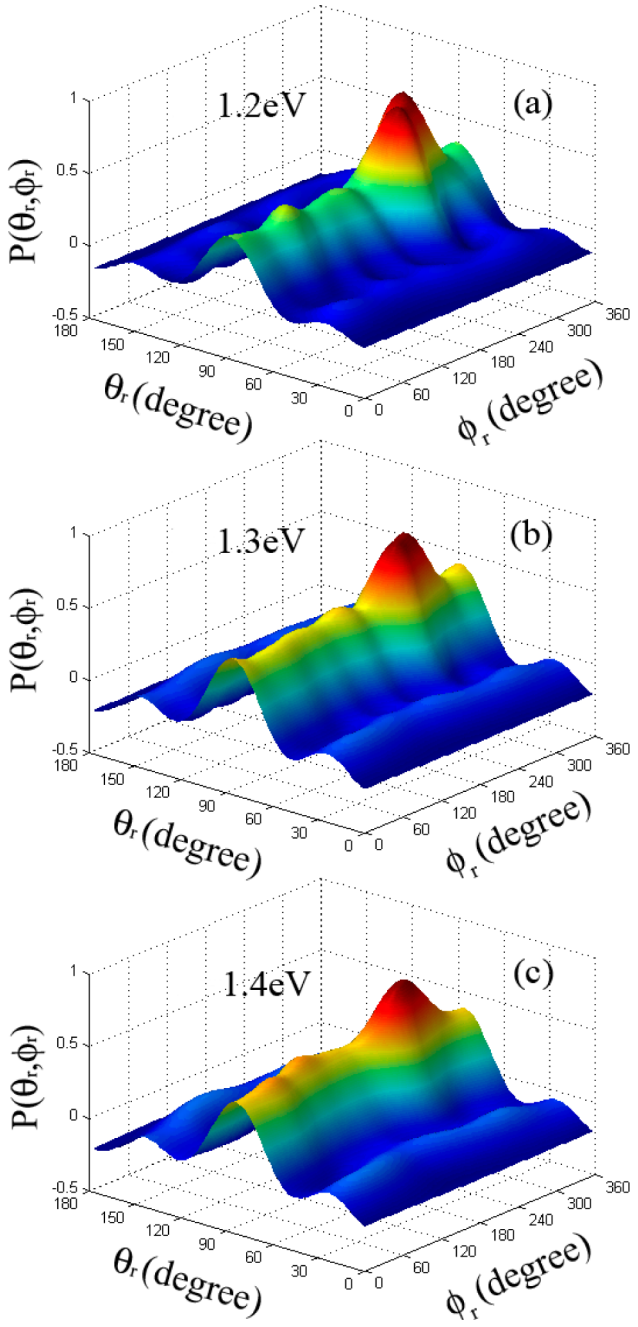

Figure 8. The angular momentum polarization distribution of $P(\theta_r,\phi_r)$ at (a) 1.2, (b) 1.3, and (c) 1.4 eV as functions of θ_r and ϕ_r for the reaction S + HD(ν = 0,j = 0) → SD + H calculated by QCT.

changes with the collision energy increase. The surfaces are all raised along the area $\theta_r = 90°$, which indicates that the vector $\boldsymbol{j}'$ prefers to be perpendicular to $\boldsymbol{k}$. Not only that, a peak appears at ($\theta_r = 90°$, $\phi_r = 270°$); therefore, we conclude that the vector $\boldsymbol{j}'$ also tends to be oriented along the negative direction of the y axis of the CM frame. We notice that the peak at ($\theta_r = 90°$, $\phi_r = 270°$) gets lower gradually, at the same time that the area ($\theta_r = 90°$, $\phi_r = 90°$) starts to rise when the collision energy increases. This change indicates that the orientation of $\boldsymbol{j}'$ is getting weaker. Instead, SD products will align on the y axis when the collision energy gets higher.

dx.doi.org/10.1021/jp410868v | J. Phys. Chem. A 2014, 118, 55–61

4. CONCLUSION

In this work, the TDWP and QCT calculations have been carried out for the reaction S(^{3}P) + HD on the lowest (1^3A″) PES with the reactant HD ($X^1\Sigma_g^+$) rotationally and vibrationally excited. During the calculation, we find from the reaction probabilities that the SD channel is in a much advantaged position of the title reaction due to the different quality value between H and D atoms. The SD channel is in the dominant position, and from the comparison between TDWP and QCT results, no obvious quantum effect is observed. In the investigation of the title reaction with reactant HD rovibrationally excited, we find that the vibration of the HD bond will promote the proceeding of the reaction and narrow the gap in ICS between the two channels, but the rotation of HD will enlarge the gap. State-to-state DCSs are calculated, and they show significant characters of the rebound mechanism. We have also studied the vector properties of SD products for the title reaction by calculating the $P(\theta_r)$, $P(\phi_r)$, and $P(\theta_r,\phi_r)$ distributions at different collision energies, and the rotational angular momentum vector of SD prefers to orient in the negative direction of the y axis at low collision energy and align on the y axis at high collision energy.

AUTHOR INFORMATION

Corresponding Author

*E-mail: mdchen@dlut.edu.cn.

Notes

The authors declare no competing financial interest.

ACKNOWLEDGMENTS

This work was supported by the National Natural Science Foundation of China (Grant No. 11374045), the Fundamental Research Funds for the Central Universities (Grant No. DUT13ZD207), the Program for Liaoning Excellent Talents in University (Grant No. LJQ2012002), and the Program for New Century Excellent Talents in University (Grant No. NCET-12-0077).

REFERENCES

(1) Lv, S. J.; Zhang, P. Y.; He, G. Z. Time-Dependent Wave Packet Quantum Scattering Study of Reaction S(^{3}P) + H_2 → HS + H on a New Ab Initio Potential Energy Surface ^{3}A′. *Chin. J. Chem. Phys.* **2012**, *25* (3), 291−296.

(2) Lv, S. J.; Zhang, P. Y.; Han, K. L.; He, G. Z. Exact Quantum Scattering Study of the H + HS Reaction on a New Ab Initio Potential Energy Surface (HS)-S_2 (^{3}A″). *J. Chem. Phys.* **2012**, *136* (9), 094308−099316.

(3) Berteloite, C.; Lara, M.; Bergeat, A.; Le Picard, S. D.; Dayou, F.; Hickson, K. M.; Canosa, A.; Naulin, C.; Launay, J. M.; Sims, I. R.; Costes, M. Kinetics and Dynamics of the S(^{1}D$_2$) + H_2 → SH + H Reaction at Very Low Temperatures and Collision Energies. *Phys. Rev. Lett.* **2010**, *105* (20), 203201−203205.

(4) Lara, M.; Chefdeville, S.; Hickson, K. M.; Bergeat, A.; Naulin, C.; Launay, J. M.; Costes, M. Dynamics of the S(^{1}D$_2$)+HD(j=0) Reaction at Collision Energies Approaching the Cold Regime: A Stringent Test for Theory. *Phys. Rev. Lett.* **2012**, *109* (13), 133201−133206.

(5) Lara, M.; Jambrina, P. G.; Varandas, A. J. C.; Launay, J. M.; Aoiz, F. J. On the Role of Dynamical Barriers in Barrierless Reactions at Low Energies: S(^{1}D)+H_2. *J. Chem. Phys.* **2011**, *135* (13), 134313−134328.

(6) Yang, H.; Han, K. L.; Schatz, G. C.; Lee, S. H.; Liu, K.; Smith, S. C.; Hankel, M. Integral and Differential Cross Sections for the S(^{1}D)+HD Reaction Employing the Ground Adiabatic Electronic State. *Phys. Chem. Chem. Phys.* **2009**, *11* (48), 11587−11595.

(7) Yang, H. A.; Han, K. L.; Schatz, G. C.; Smith, S. C.; Hankel, M. Exact and Truncated Coriolis Coupling Calculations for the S(^{1}D) + HD Reaction Employing the Ground Adiabatic Electronic State. *Phys. Chem. Chem. Phys.* **2010**, *12* (39), 12711−12718.

(8) Ho, T. S.; Hollebeek, T.; Rabitz, H.; Der Chao, S.; Skodje, R. T.; Zyubin, A. S.; Mebel, A. M. A Globally Smooth Ab Initio Potential Surface of the ^{1}A′ State for the Reaction S(^{1}D)+H_2. *J. Chem. Phys.* **2002**, *116* (10), 4124−4134.

(9) Su, Y.; Kang, L. H. A Comparison of the Stereo-Dynamical Information Between S(^{1}D) + H_2 and S(^{1}D) + HD Reactions. *Comput. Theor. Chem.* **2012**, *1002* (0), 9−15.

(10) Olschewski, H. A.; Troe, J.; Wagner, H. G. UV Absorption Study of the Thermal-Decomposition Reaction H_2S → H_2 + S(^{3}P). *J. Phys. Chem.* **1994**, *98* (49), 12964−12967.

(11) Shiina, H.; Oya, M.; Yamashita, K.; Miyoshi, A.; Matsui, H. Kinetic Studies on the Pyrolysis of H_2S. *J. Phys. Chem.* **1996**, *100* (6), 2136−2140.

(12) Maiti, B.; Schatz, G. C.; Lendvay, G. Importance of Intersystem Crossing in the S(^{3}P,^{1}D) + H_2 → SH + H Reaction. *J. Phys. Chem. A* **2004**, *108* (41), 8772−8781.

(13) Chu, T. S.; Zhang, Y.; Han, K. L. The Time-Dependent Quantum Wave Packet Approach to the Electronically Nonadiabatic Processes in Chemical Reactions. *Int. Rev. Phys. Chem.* **2006**, *25* (1−2), 201−235.

(14) Chu, T. S.; Han, K. L. Effect of Coriolis Coupling in Chemical Reaction Dynamics. *Phys. Chem. Chem. Phys.* **2008**, *10* (18), 2431−2441.

(15) Chu, T. S.; Zhang, X.; Han, K. L. A Quantum Wave-Packet Study of Intersystem Crossing Effects in the O(^{3}P$_{2,1,0}$,^{1}D$_2$)+H_2 Reaction. *J. Chem. Phys.* **2005**, *122* (21), 214301−214307.

(16) Chu, T. S.; Han, K. L.; Schatz, G. C. Significant Nonadiabatic Effects in the S(^{1}D)+HD Reaction. *J. Phys. Chem. A* **2007**, *111* (34), 8286−8290.

(17) Chen, M. D.; Tang, B. Y.; Han, K. L.; Lou, N. Q.; Zhang, J. Z. H. Accurate Quantum Mechanical Calculation for the N+OH Reaction. *J. Chem. Phys.* **2003**, *118* (15), 6852−6857.

(18) Xu, X. S.; Zhang, W. Q.; Duan, L. H.; Chen, M. D. Quasi-Classical Trajectory Study of Stereodynamics for the O + HCl → OH + Cl Reaction. *Chem. J. Chin. Univ.* **2010**, *31* (5), 1034−1038.

(19) Fleck, J. A.; Morris, J. R.; Feit, M. D. Time-Dependent Propagation of High-Energy Laser-Beams through Atmosphere. *Appl. Phys.* **1976**, *10* (2), 129−160.

(20) Sun, Z. G.; Zhang, D. H. State-to-State Reactive Scattering by Quantum Wavepacket Method. *Prog. Chem.* **2012**, *24* (6), 1153−1165.

(21) Sun, Z. G.; Yang, W. T.; Zhang, D. H. Higher-Order Split Operator Schemes for Solving the Schrodinger Equation in the Time-Dependent Wave Packet Method: Applications to Triatomic Reactive Scattering Calculations. *Phys. Chem. Chem. Phys.* **2012**, *14* (6), 1827−1845.

(22) Light, J. C.; Carrington, T. Discrete-Variable Representations and Their Utilization. *Adv. Chem. Phys.* **2000**, *114*, 263−310.

(23) Sun, Z. G.; Lee, S. Y.; Guo, H.; Zhang, D. H. Comparison of Second-Order Split Operator and Chebyshev Propagator in Wave Packet Based State-to-State Reactive Scattering Calculations. *J. Chem. Phys.* **2009**, *130* (17), 174102.

(24) Peng, T.; Zhu, W.; Wang, D. Y.; Zhang, J. Z. H. Reactant−Product Decoupling Approach to State-to-State Dynamics Calculation for Bimolecular Reaction and Unimolecular Fragmentation. *Faraday Discuss.* **1998**, *110*, 159−167.

(25) Sun, Z. G.; Zhang, D. H.; Alexander, M. H. Time-Dependent Wavepacket Investigation of State-to-State Reactive Scattering of Cl with para-H_2 Including the Open-Shell Character of the Cl Atom. *J. Chem. Phys.* **2010**, *132* (3), 034308.

(26) Zhang, J. Z. H.; Miller, W. H. Quantum Reactive Scattering via the S-Matrix Version of the Kohn Variational Principle — Differential and Integral Cross-Sections for D+H_2 → HD+H. *J. Chem. Phys.* **1989**, *91* (3), 1528−1547.

(27) Cheng, D.; Yang, T.; Chen, M. Stereodynamics Study of the Abstraction Reaction H + CD_4 → HD + CD_3. *J. Theor. Comput. Chem.* **2013**, *12* (02), 1250109.
(28) Han, K. L.; He, G. Z.; Lou, N. Q. Effect of Location of Energy Barrier on the Product Alignment of Reaction A+BC. *J. Chem. Phys.* **1996**, *105* (19), 8699−8704.
(29) Zhang, W. Q.; Li, Y. Z.; Xu, X. S.; Chen, M. D. Isotope Effects on the Dynamics in the Ion−Diatomic Collisions of D^+, H^+ with H_2 and D_2 Molecules. *Chem. Phys.* **2010**, *367* (2−3), 115−119.
(30) Chen, M. D.; Han, K. L.; Lou, N. Q. Theoretical Study of Stereodynamics for the Reactions Cl+H_2/HD/D_2. *J. Chem. Phys.* **2003**, *118* (10), 4463−4470.
(31) Zhang, W. Q.; Cong, S. L.; Zhang, C. H.; Xu, X. S.; Chen, M. D. Theoretical Study of Dynamics for the Abstraction Reaction H′ + HBr(ν = 0, j = 0) → H′H + Br. *J. Phys. Chem. A* **2009**, *113* (16), 4192−4197.
(32) Zhang, W. Q.; Chen, M. D. Quasiclassical Trajectory Study of the Stereodynamics for the Reaction D^+ + H_2 (ν = 0,j = 0) → HD + H^+. *J. Theor. Comput. Chem.* **2009**, *8* (6), 1131−1141.
(33) Polanyi, J. C.; Wong, W. H. Location of Energy Barriers. I. Effect on Dynamics of Reactions A+BC. *J. Chem. Phys.* **1969**, *51* (4), 1439−1450.
(34) Lv, S. J.; Zhang, P. Y.; Zhao, M. Y.; He, G. Z. Quantum Wave Packet Dynamics Study of the S(^{3}P) + H_2 Reaction on the Lowest SH_2($^1A_3''$) State. *Comput. Theor. Chem.* **2012**, *997* (0), 83−87.

dx.doi.org/10.1021/jp410868v | *J. Phys. Chem. A* 2014, 118, 55−61